Journal of Inorganic Biochemistry 210 (2020) 111161

Contents lists available at ScienceDirect

Journal of Inorganic Biochemistry

journal homepage: www.elsevier.com/locate/jinorgbio

Short Communication

Protein dynamics of [Cu-Zn] superoxide dismutase (SOD1): How protein motions at the global and local levels impact the reactivity of SOD1

Eamonn F. Healy[a,*], Rafael Flores[a], Vincent M. Lynch[b], Santiago Toledo[a,*]

[a] Department of Chemistry, St. Edward's University, Austin, TX 78704, USA
[b] Department of Chemistry, The University of Texas at Austin, Austin, TX 78712, USA

ARTICLE INFO

Keywords:
Superoxide dusmutase
SOD1
Biomimetic model
Normal mode analysis
Protein motion

ABSTRACT

This work explores the pivotal role that protein mobility plays in facilitating the catalytic activity of Copper-Zinc superoxide dismutase (SOD1). Through both localized active site distortions and correlated domain movement, these motions enable the enzyme to adopt the conformations necessary to achieve both substrate delivery and efficient catalytic transformation. Structural and computational studies of a biomimetic model complex are used to probe the localized interactions between substrate and secondary sphere residues that play a role in guiding substrate to the active site, as well as facilitating the conformational changes necessary for substrate turnover. Normal mode analysis (NMA) of SOD1 demonstrates how collective domain motion influences key residues of the electrostatic loop (ESL), guiding substrate to the active site and facilitating the delivery of the conserved water network necessary for proton transfer.

The mechanism for disproportionation of the toxic superoxide radical anion by [Cu-Zn] superoxide dismutase (SOD1) involves cyclic reduction and oxidation of the catalytic copper to produce oxygen and hydrogen peroxide [1]. In the resting state the Cu^{2+} ion forms a tetracoordinated distorted tetrahedron (td) coordinated by N_δ of His_{46}, the N_ε atoms of His_{48} and His_{120}, and N_ε of deprotonated His_{63} (human SOD1 numbering) [2]. The reduction to Cu^{+} is accompanied by a displacement of the metal away from now protonated His_{63} and towards the trigonal plane formed by histidines 46, 48 and 120. Anion binding studies support a mechanism whereby direct binding of superoxide to Cu^{2+} yields a five-coordinate square pyramidal geometry with a loosely-bound apical His_{48} residue [3]. Subsequent inner-sphere electron transfer is promoted by proton transfer through a chain of conserved water molecules positioned along an active site channel [4]. The extent to which protein motions are involved in enzymatic turnover is the focus of intense investigation [5], and the importance of SOD1 mobility in facilitating catalytic activity as well as aberrant behavior has been suggested by both structural [6] and theoretical [7] investigations. This work combines both model structure and theoretical analysis of ligand binding to SOD1 in order to elucidate how collective motions, both local and global, in the SOD1 protein can act in a correlated manner to influence both conformational changes at the catalytic center and substrate delivery to the active site.

The model complex, $[Cu(II)(isobpmen)(H_2O)](OTf)_2$, was synthesized and isolated in good yield from the complexation of *N*,*N*-Bis(2-pyridylmethyl)-N′,*N*′-dimethylethane-1,2-di-amine (isobpmen) ligand and copper(*II*)triflate. The precursor ligand was synthesized via reductive amination of *N*,*N*-dimethylethylenediamine with two equivalents of 2-pyridinecarboxaldehyde (see supporting information for details). Blue needle shaped crystals resulted from the complexation and the ORTEP structural diagram of complex 1 is shown in Fig. 1A and S4. Complex 1 displays a square pyramidal geometry coordinated by two tertiary amine nitrogens, one of them elongated trans to the open site, and two ligating pyridines. The fifth ligand is a water bound molecule. One of the triflate (Tf) counterions displays a strong hydrogen bonding interaction to the water ligand with a H_{H2O}-O_{OTf} distance of 1.86 Å. This interaction can be visualized by looking at the interface between the triflate with the Hirshfeld surface of the complex, as mapped over the normalized contact distance, d_{norm} [8]. The intense red spot in Fig. 2 corresponds to an H_{H2O}-O_{OTf} distance closer than the sum of the Van-der-Waals radii due to a hydrogen bond contact. Density functional theory (DFT) calculations using a triple-zeta (TZV) basis set and the B3LYP functional were performed on the $[Cu(II)(isobpmen)(H_2O)]^{2+}$ complex in the absence of the triflate counterions (Fig. 1B and S5). The optimized geometry highlights how, absent the triflate, the geometry of the complex is predicted to be trigonal bipyramidal (tbp), with a $N_{py}Cu(II)N_{py}$ angle of 116.4°, compared to 155.8° in the crystal structure.

As mentioned above, binding of anion substrate analogues such as

* Corresponding author.
E-mail address: healy@stedwards.edu (E.F. Healy).

https://doi.org/10.1016/j.jinorgbio.2020.111161
Received 17 April 2020; Received in revised form 18 May 2020; Accepted 12 June 2020
Available online 24 June 2020
0162-0134/

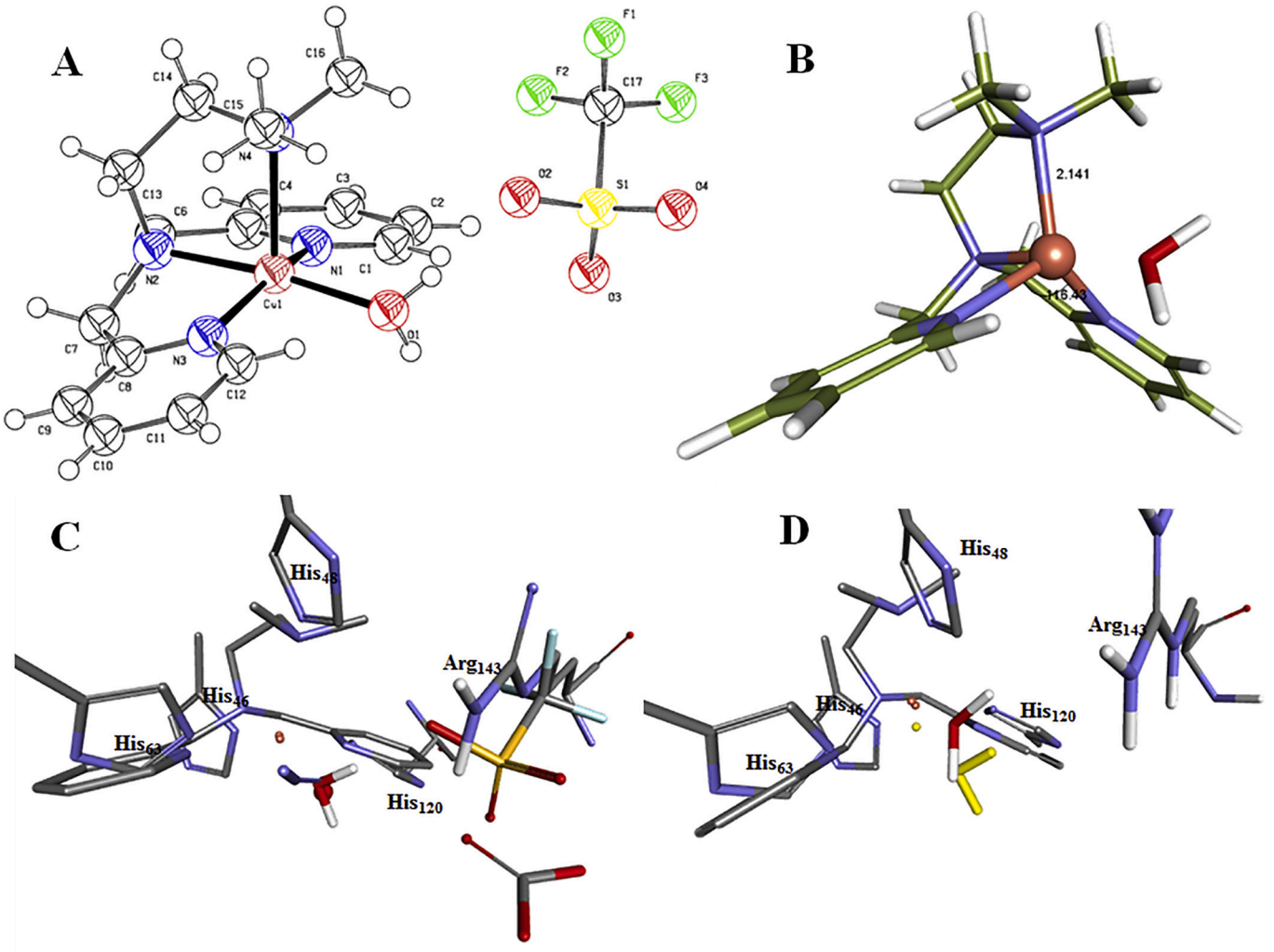

Fig. 1. A Crystal structure of [Cu(II)(isobpmen)(H_2O)]($OTf)_2$; **B** structure of [Cu(II)(isobpmen)(H_2O)]$^{2+}$ complex optimized using a triple-zeta (TZV) basis set and the B3LYP functional; **C** alignment of [Cu(II)(isobpmen)(H_2O)]($OTf)_2$ with the azide (blue stick)-bound SOD1 structure from Ref. [3], and showing conserved water W_0 (red ball), and HCO_3^- ligand (stick) from the Cu(II)-carbonate bound structure from Ref [8]; **D** alignment of the DFT-optimized structure of [Cu(II)(isobpmen)(H_2O)]$^{2+}$with the fully oxidized subunit of bovine SOD1 from Ref. [12], with the Cu^{2+} and the water from the [Cu(II)(isobpmen)(H_2O)]($OTf)_2$ complex overlaid in yellow.

azide to oxidized SOD1 changes the Cu^{2+} coordination to a five-coordinate square pyramidal geometry with His_{48} occupying an axial position, loosely coupled at a N^{ε}-Cu^{2+} distance of 2.76 Å. The ligating azide nitrogen displaces a conserved water molecule, W_0, which represents the binding site of the superoxide substrate. As can be seen from the alignment of our model compound with the azide-bound SOD1 structure, Fig. 1C, our ligating water has the same relationship to the metal center as does the ligating azide nitrogen. Also shown in Fig. 1C is the conserved water, W_0, from a carbonate-bound SOD1 complex where the HCO_3^- ligand occupies a position proximate to Arg_{143} [9]. The guanidium group of Arg_{143} is known to play a critical role in contributing to the local electrostatic environment necessary for the binding of anions, including the superoxide substrate [10], azide and thiocyanate ligands [11], and the bicarbonate anion [9]. The alignment in Fig. 1C highlights how the triflate counterion plays a role analogous to that of Arg_{143} in SOD1. By contrast alignment of the DFT-optimized structure with a fully oxidized subunit of bovine SOD1 [12], Fig. 1D, demonstrates how absent the counterion the Cu^{2+} position in the model compound reflects the tetrahedral orientation of the four ligating histidines typical of oxidized resting state SOD1. Therefore just as hydrogen bonding between the water and the triflate converts the conformation in the model compound from tbp to square pyramidal, so electrostatic guidance of the anionic substrate by Arg_{143} in SOD1 results in a change in metal coordination from distorted td to square pyramidal. In SOD1 these coordination changes are required for copper to engage catalytic activity and facilitated by protein motion.

Normal mode analysis (NMA) describes protein movement as a superposition of mode coordinates, with the majority of protein motion attributable to one or two of the lowest frequency modes [13]. For wtSOD1, NMA yields two low frequency modes with substantial collective character. Frames from a movie (available as supplementary material) depicting one of these modes, Fig. 3 (available as a supplementary figure in the web version of this article), demonstrates how the collective motion of SOD1 facilitates a displacement of the Cu^{2+} center relative to the ligating histidines. Specifically, a reduction of the $_{His63}N^{\varepsilon}$-Cu^{2+}- $N^{\varepsilon}{}_{His120}$ angle is associated with a contraction of the Cu^{2+}- N^{ε}_{His48} distance, while a looser attachment of His_{48} is associated with a copper ion coplanar with the three remaining histidines. This collective motion thus provides a mechanism to transition the metal from the tetrahedral arrangement associated with unbound substrate to the square pyramidal geometry observed with ligand binding. For the model compound the Lewis basicity of the ligating oxygen is increased through polarization and charge transfer [14], thus favoring the square pyramidal conformation. The alignment in Fig. 1C highlights how a

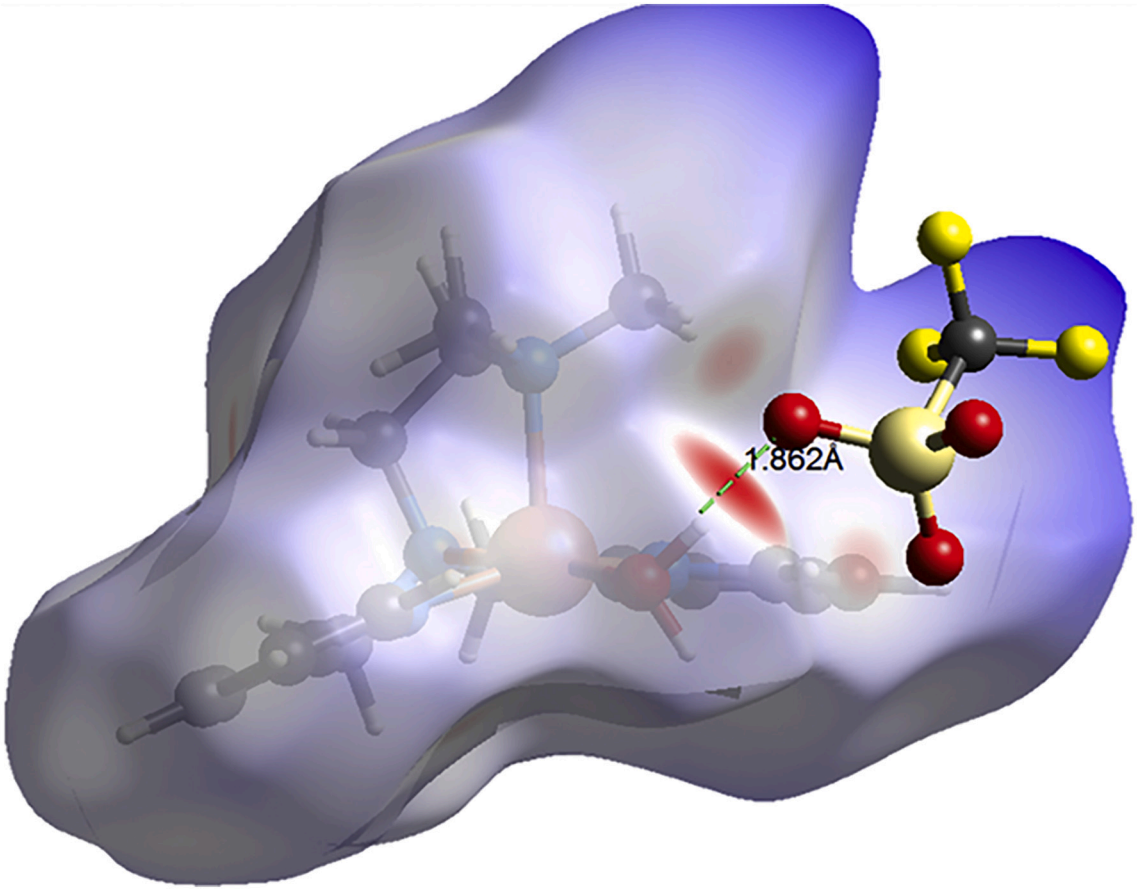

Fig. 2. Hirshfeld surface of the [Cu(II)(isobpmen)(H_2O)]($OTf)_2$ complex, as mapped over the normalized contact distance, d_{norm}, with a red spot signifying a distance closer than the sum of the Van-der-Waals radii.

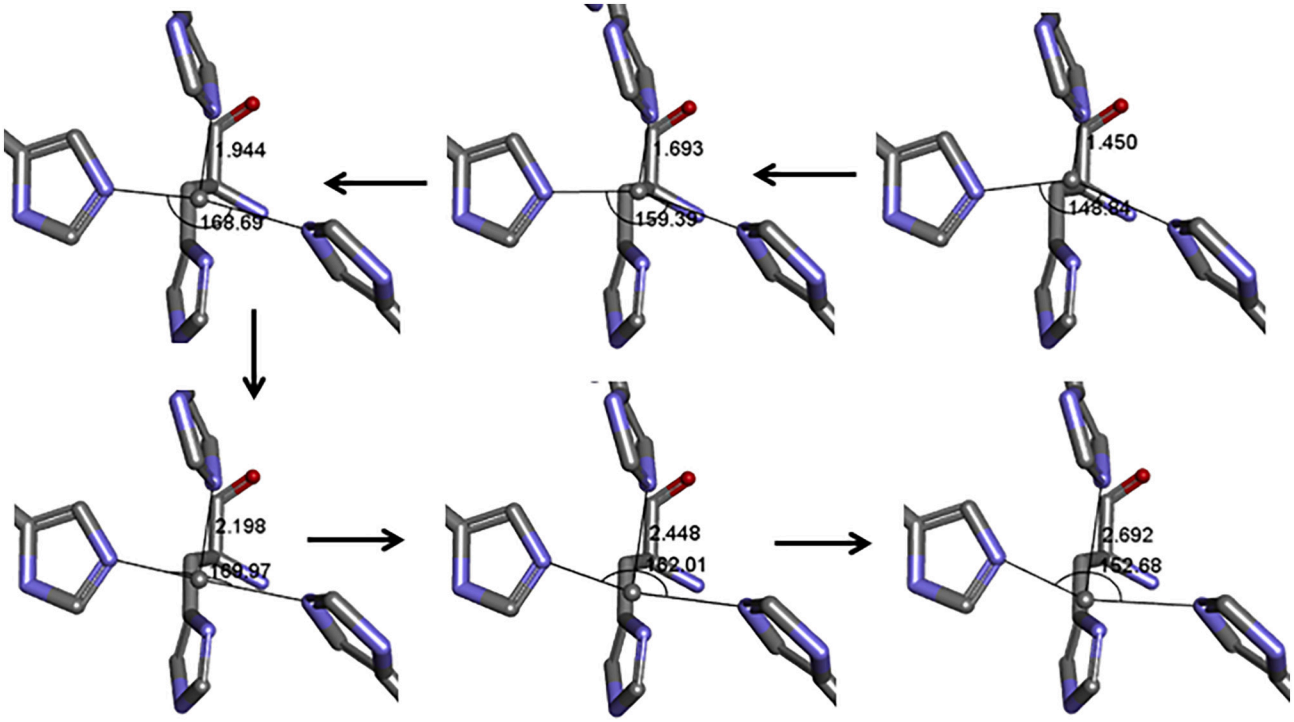

Fig. 3.

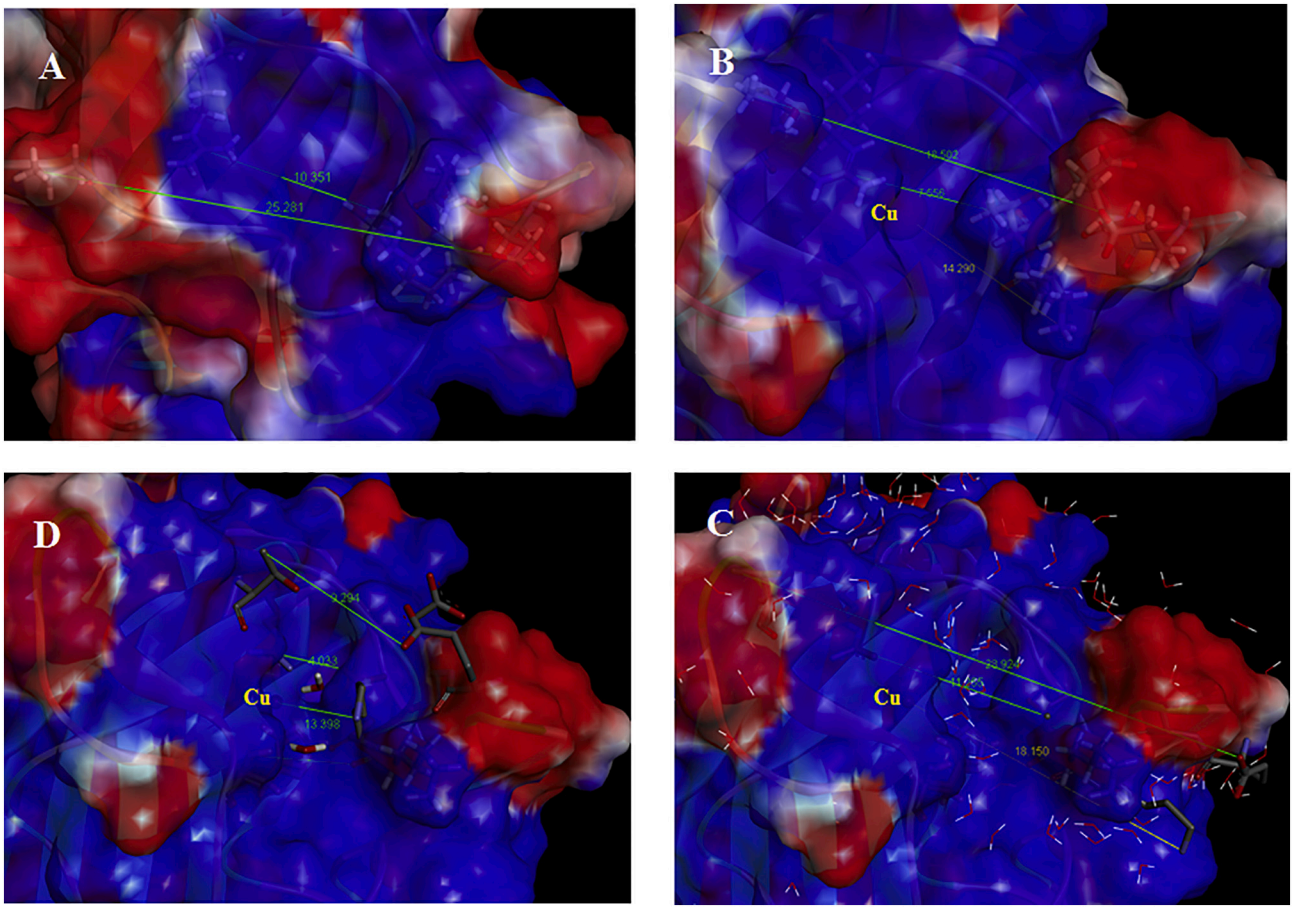

Fig. 4. A Surface electrostatic potentials calculated using the Discovery Studio software for copper-free SOD1(pdb id 1KMG) and **B** wt SOD1 (pdb id 2C9V) with positive regions in blue and negative charges in red (kt units); **C** & **D** Surface electrostatic potential for wtSOD1 overlaid with initial and final frames respectively (stick mode) of the motion described by bimodal NMA analysis involving the two modes with the lowest calculated frequencies and the largest collective character, with the crystallographic waters shown in wireframe in **C**, and the conserved waters W_0 and W_2 shown in stick in **D**. (For interpretation of the references to colour in this figure legend, the reader is referred to the web version of this article.)

similar orientation of Arg_{143} relative to superoxide, and facilitated by protein motion, utilizes electrostatic guidance to achieve the same conversion. The active-site Cu^{2+} ion sits at the bottom of a deep but narrow channel formed on one side by the residues of loop IV, often termed the zinc-binding loop (ZBL), and on the other by loop VII or the electrostatic loop (ESL). Superimposing both low frequency normal modes demonstrates how protein motion in SOD1 can also produce a longer-range electrostatic effect, one that guides anionic substrates along this active site, or electrostatic channel, and facilitate proton transfer from solution [15]. Defining the length of the electrostatic channel as the distance from the copper to N_ξ of Lys_{136} and its width as the distance from C_γ of Thr_{58} to the O_ε atom of Glu_{132} [16], it can be seen from Fig. 4A and B how the binding of copper is critical to the formation of a well-defined channel through correct orientation of key residue side chains. In Fig. 4C one frame of this bimodal movement is overlaid with the electrostatic surface calculated for wtSOD1 (pdb id 2C9V) to demonstrate how the predicted motion of the protein expands the size of the channel in a manner similar to that observed in the absence of the copper center (apoprotein). Because normal modes define direction but not amplitude, an amplitude range was specified to capture larger amplitude protein motions while allowing for a reasonable comparison with experimental B factors. B factors were computed by a linear scaling of the relationship $B = (8\pi^2/3) < R^2 >$ where $< R^2 >$ is the root mean square displacement of the 100 lowest frequencies. For the residues from loops IV and VII lining the channel, the correlation between computed and observed B-factors was calculated to be 0.91, Fig. S6. Therefore, while metalation of SOD1 orients key side chains to give a well-defined electrostatic channel, NMA describes a more dynamic environment where residual mobility permits fluctuations in the electrostatic environment of the active site.

The terminal frame of the bimodal movement, a motion leading to a restriction of the channel, is shown in Fig. 4D overlaid with the calculated electrostatic surface for wtSOD1. Also shown, in stick form, are two crystallographic waters including W_0, the proxy for superoxide. This protein motion facilitates electrostatic guidance of SOD1 substrate to the catalytic center through a sweeping motion of the Lys_{136} residue along the active channel, as well as a pinching of the bottleneck in the channel as defined by the distance between C_ξ of Arg_{143} and C_γ of Thr_{137} [16]. Facilitated by the localized motion of the Cu^{2+} center relative to the ligating histidines, oxidation of superoxide to O_2 is accompanied by proton transfer from bulk solvent to His_{63}, while reduction of superoxide to H_2O_2 must be accompanied by proton transfer from both solvent and from His_{63}. A conserved water network, characterized as $W_0/W_1/W_2$, is proposed as the proton source, with W_2 anchored in place by hydrogen bonding to the amide nitrogen of His_{63} and the oxygen of Lys_{136} [9]. The second crystallographic water highlighted in Fig. 4D is positioned between the His_{63} and Lys_{136} residues in the final frame of the bimodal motion of SOD1 predicted by NMA, demonstrating how collective motion can be used not just to guide substrate to the active site, but also for the delivery of a conserved water network proximate to the catalytic center. Pulse-radiolytic measurements confirm the key roles played by Lys_{136} and Arg_{143} in influencing SOD1 reactivity through modulation of the electrostatic environment [10,17]. While charge reversal through mutation of Lys_{136}

lowers SOD1 reactivity by 50%, mutation of Arg_{143} to aspartate or glutamate decreased activity by two orders of magnitude. Ionic strength is also dominated by Arg_{143}, where the charge neutralization drops the ionic dependence to 25%, compared to 75% for Lys_{136}. The protein motion described here for SOD1 explains how both residues combine to modulate the long-range electrostatic environment, but only Arg_{143} impacts the local electrostatic environment vital to the enzyme mechanism.

Secondary sphere interactions responsible for substrate focusing in the model complex $[Cu(II)(isobpmen)(H_2O)](OTf)_2$ illustrate how the conformational changes necessary for catalytic activity in SOD1 are promoted by protein movement. Global protein motion centered on the electrostatic channel of the enzyme is proposed to act synergistically with changes at the active site to concertedly impact catalytic action. This connection of protein dynamics to SOD1 catalytic activity extends beyond just action along a local reaction coordinate to include motions that accelerate delivery of substrate and proton transfer from the bulk solvent.

Electronic Supplementary Information (ESI) available: includes details of all experiments and theoretical calculations, and a movie of the normal mode, shown in Fig. 3, that demonstrates how the collective motion of SOD1 facilitates a displacement of the Cu^{2+} center relative to the ligating histidines. Supplementary data to this article can be found online at https://doi.org/10.1016/j.jinorgbio.2020.111161.

Credit authorship contribution statement

Eamonn F. Healy: Conceptualization, Methodology, Visualization, Formal analysis, Data curation, Writing - original draft, review & editing. **Rafael Flores**: Investigation. **Vincent M. Lynch**: Investigation. **Santiago Toledo**: Conceptualization, Methodology, Supervision, Validation, Writing - original draft, review & editing, Funding acquisition.

Declaration of competing interest

The authors declare that they have no known competing financial interests or personal relationships that could have appeared to influence the work reported in this paper.

Acknowledgement

The authors wish to acknowledge the support of the National Institute of General Medical Sciences of the National Institutes of Health (SC2GM130438), the National Science Foundation (#1832282), as well as Welch Foundation (Grant# BH-0018) for its continuing support of the Chemistry Department at St. Edward's University. This work used the Extreme Science and Engineering Discovery Environment (XSEDE), which is supported by National Science Foundation grant number ACI-1548562.

References

[1] I.A. Abreu, D.E. Cabelli, Superoxide dismutases—a review of the metal-associated mechanistic variations, Biochim. Biophys. Acta, Proteins Proteomics 1804 (2010) 263–274.
[2] J.S. Valentine, P.A. Doucette, S. Zittin Potter, Copper-zinc superoxide dismutase and amyotrophic lateral sclerosis, Annu. Rev. Biochem. 74 (2005) 563–593.
[3] P.J. Hart, M.M. Balbirnie, N.L. Ogihara, A.M. Nersissian, M.S. Weiss, J.S. Valentine, D. Eisenberg, A structure-based mechanism for copper − zinc superoxide dismutase, Biochemistry 38 (1999) 2167–2178.
[4] V.V. Smirnov, J.P. Roth, Mechanisms of electron transfer in catalysis by copper zinc superoxide dismutase, J. Am. Chem. Soc. 128 (2006) 16424–16425.
[5] V.C. Nashine, S. Hammes-Schiffer, S.J. Benkovic, Coupled motions in enzyme catalysis, Curr. Opin. Chem. Biol. 14 (2010) 644–651.
[6] M.A. Hough, R.W. Strange, S.S. Hasnain, Conformational variability of the cu site in one subunit of bovine CuZn superoxide dismutase: the importance of mobility in the Glu119-Leu142 loop region for catalytic function, J. Mol. Biol. 304 (2000) 231–241.
[7] E.F. Healy, A. Roth-Rodriguez, S. Toledo, A model for gain of function in superoxide dismutase *Biochem*, Biochem. Biophys. Rep. 21 (2020) 100728.
[8] M.A. Spackman, D. Jayatilaka, Hirshfeld surface analysis, CrystEngComm 11 (2009) 19–32.
[9] R.W. Strange, M.A. Hough, S.V. Antonyuk, S.S. Hasnain, Structural evidence for a copper-bound carbonate intermediate in the peroxidase and dismutase activities of superoxide dismutase, PLoS One 7 (2012) e44811.
[10] C.L. Fisher, D.E. Cabelli, J.A. Tainer, R.A. Hallewell, E.D. Getzoff, The role of arginine 143 in the electrostatics and mechanism of Cu, Zn superoxide dismutase: computational and experimental evaluation by mutational analysis, Proteins: Struct., Funct., Bioinf. 19 (1994) 24–34.
[11] M. Leone, A. Cupane, V. Militello, M.E. Stroppolo, A. Desideri, Fourier transform infrared analysis of the interaction of azide with the active site of oxidized and reduced bovine Cu, Zn superoxide dismutase, Biochemistry 37 (1998) 4459–4464.
[12] M.A. Hough, S.S. Hasnain, Crystallographic structures of bovine copper-zinc superoxide dismutase reveal asymmetry in two subunits: functionally important three and five coordinate copper sites captured in the same crystal, J. Mol. Biol. 287 (1999) 579–592.
[13] K. Suhre, Y.H. Sanejouand, ElNemo: a normal mode web server for protein movement analysis and the generation of templates for molecular replacement, Nucleic Acids Res. 32 (suppl_2) (2004) W610–W614.
[14] E. Ramos-Cordoba, D.S. Lambrecht, M. Head-Gordon, Charge-transfer and the hydrogen bond: spectroscopic and structural implications from electronic structure calculations, Faraday Discuss. 150 (2011) 345–362.
[15] R.W. Strange, S.V. Antonyuk, M.A. Hough, P.A. Doucette, J.S. Valentine, S.S. Hasnain, Variable metallation of human superoxide dismutase: atomic resolution crystal structures of Cu–Zn, Zn–Zn and as-isolated wild-type enzymes, J. Mol. Biol. 356 (2006) 1152–1162.
[16] L. Banci, I. Bertini, F. Cantini, M. D'Onofrio, M.S. Viezzoli, Structure and dynamics of copper-free SOD: the protein before binding copper, Protein Sci. 11 (2002) 2479–2492.
[17] C.L. Fisher, D.E. Cabelli, R.A. Hallewell, P. Beroza, T.P. Lo, E.D. Getzoff, J.A. Tainer, Computational, pulse-radiolytic, and structural investigations of lysine-136 and its role in the electrostatic triad of human Cu, Zn superoxide dismutase, Proteins Struct. Funct. Genet. 29 (1997) 103–112.